Effects of Dopamine and Glutamate on Synaptic Plasticity: A Computational Modeling Approach for Drug Abuse as Comorbidity in Mood Disorders

Authors

Z. Qi[1,2,3], S. Kikuchi[1,3], F. Tretter[4], E. O. Voit[1,3]

Affiliations

[1] Department of Biomedical Engineering, Georgia Institute of Technology and Emory University Medical School, Atlanta, GA, USA
[2] Center for Neurodegenerative Disease, Emory University School of Medicine, Atlanta, GA, USA
[3] Integrative BioSystems Institute, Georgia Institute of Technology, Atlanta, GA, USA
[4] Isar-Amper-Klinikum gemeinnützige GmbH, Klinikum München-Ost, Haar, Landkreis München, Germany

Abstract

Major depressive disorder (MDD) affects about 16% of the general population and is a leading cause of death in the United States and around the world. Aggravating the situation is the fact that "drug use disorders" are highly comorbid in MDD patients, and *vice versa*. Drug use and MDD share a common component, the dopamine system, which is critical in many motivation and reward processes, as well as in the regulation of stress responses in MDD. A potentiating mechanism in drug use disorders appears to be synaptic plasticity, which is regulated by dopamine transmission. In this article, we describe a computational model of the synaptic plasticity of GABAergic medium spiny neurons in the nucleus accumbens, which is critical in the reward system. The model accounts for effects of both dopamine and glutamate transmission. Model simulations show that GABAergic medium spiny neurons tend to respond to dopamine stimuli with synaptic potentiation and to glutamate signals with synaptic depression. Concurrent dopamine and glutamate signals cause various types of synaptic plasticity, depending on input scenarios. Interestingly, the model shows that a single 0.5 mg/kg dose of amphetamine can cause synaptic potentiation for over 2 h, a phenomenon that makes synaptic plasticity of medium spiny neurons behave quasi as a bistable system. The model also identifies mechanisms that could potentially be critical to correcting modifications of synaptic plasticity caused by drugs in MDD patients. An example is the feedback loop between protein kinase A, phosphodiesterase, and the second messenger cAMP in the postsynapse. Since reward mechanisms activated by psychostimulants could be crucial in establishing addiction comorbidity in patients with MDD, this model might become an aid for identifying and targeting specific modules within the reward system and lead to a better understanding and potential treatment of comorbid drug use disorders in MDD.

Bibliography
DOI http://dx.doi.org/10.1055/s-0031-1273707
Pharmacopsychiatry 2011; 44 (Suppl. 1): S62–S75

ISSN 0176-3679

Correspondence
E. O. Voit, PhD
313 Ferst Drive
Department of Biomedical Engineering
GA 30332-0535 Atlanta
USA
Tel.: +1/404/385 5057
Fax: +1/404/894 4243
eberhard.voit@bme.gatech.edu

Introduction

Mood disorder is mainly characterized by a disturbance in a patient's mental well-being and includes major depressive disorder (MDD) and bipolar disorder. MDD is regarded as a leading cause of death world-wide with an estimated prevalence of 16% in the United States [26, 39]. Neuropsychiatry already has identified several macroanatomic brain structures and circuits by imaging studies and deep brain stimulation that are involved in the clinical phenomenology of mood disorders [3, 13, 35–38, 47]: the prefrontal cortex that is responsible for impaired cognitive operations, the nucleus accumbens that is related to loss of hedonic states, the hippocampus with its memory dysfunctions, the striatal complex that is involved in reduced psychomotor action, the orbitofrontal cortex that exhibits reduced behavioral inhibition, and the amygdala that is related to elevated impulsive behavior (**Fig. 1a**). In addition, pharmacological studies have shown that several transmitter systems are involved in the symptomatology of depressive disorders. Deficits in norepinephrinergic, serotonergic and dopaminergic neurotransmission are well known [65], a hyperfunction of the cholinergic system was proposed [24], and lately also a GABA hypofunction hypothesis and a glutamate hyperfunction hypothesis were discussed [30, 32, 60]. Although the etiology of MDD is not well understood, it has been suggested from a biochemical point of view that monoamines and the hypothalamic-pituitary-adrenal (HPA) axis in human brain are important contributors [33, 53]. Briefly, the HPA axis responds to stress with the release

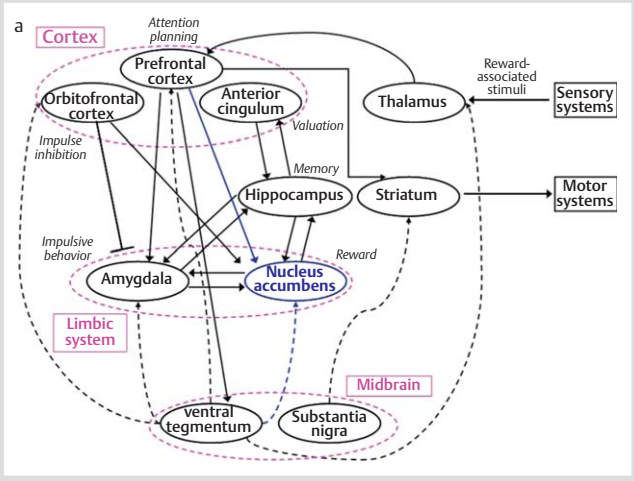

Fig. 1a Macroanatomic brain circuitry related to symptoms of depression as a local malfunctioning of certain brain regions. The diagram shows the main focus of the computational modeling study, namely the nucleus accumbens and its associated projections from the ventral tegmental area and the prefrontal cortex (highlighted in blue). Dashed arrows: dopamine projections. Anterior cingulum = anterior cingulated cortex, ventral tegmentum = ventral tegmental area.

of pro-inflammatory cytokines. The stress response is regulated by the monoamine system, and disturbed monoamine transmission therefore impairs the regulation of stress responses. Thus, functional disorders of monoamine transmission, the HPA axis, and stress together contribute to MDD [51].

Two types of monoamines, norepinephrine and serotonin, have been the primary subject of investigation in the context of MDD. In comparison, dopamine (DA) has attracted less attention, although DA transmission is very important for the disorder as well. For instance, one of the 2 required symptoms of MDD in the criteria of the *Diagnostic and Statistical Manual of Mental Disorders* [1] is anhedonia with a prevalence of almost 40% among MDD patients [46]. Anhedonia is the inability to experience enjoyment from activities that had been pleasurable before, and a reduction in DA transmission in the nucleus accumbens has been suggested as the cause [3,38,75–77]. Because DA plays an important role in motivation and reward, the reduction in DA transmission, and the correspondingly reduced reward, can directly contribute to comorbidity between drug use and MDD [42]. Indeed, this association has been reported for quite some while [9,58,59]: MDD is diagnosed in about 30% of cocaine addicts, and about 10% of MDD patients have drug use disorders [61,73].

Different causalities have been suggested for the interaction between drug use disorders and a depressive disorder. One hypothesis suggests that neuronal adaptation is caused by chronic drug use due to frequent over-stimulation of brain reward pathways, and that drug withdrawal can therefore lead to depressive symptoms such as anhedonia [10,16]. Another possible causality (called the *self-medication hypothesis*) is that use of psychostimulants by MDD patients is an intentional strategy for improving their mental states [27,34]. Other suggested mechanisms purport that drug use causes stress which then induces MDD or that drug use disorders share specific underlying processes with MDD. Such mechanisms are far from clear and may be complicated. However, these disorders have the DA system in common. In addition to the critical roles of DA in motivation and reward, as well as its contribution to anhedonia, indirect support for the involvement of DA comes from pharmacological observations. Reserpine depletes monoamine and can cause depressive symptoms in some patients. Iproniazid inhibits the degradation of monoamine by monoamine oxidase and improves depressive moods, while imipramine blocks the reuptake of monoamine and can have an antidepressant effect. While these observations are mainly associated with norepinephrine and serotonin, DA also belongs to the class of monoamines and shares almost the same metabolic pathway with norepinephrine. In fact, DA is the precursor of norepinephrine. Thus, antidepressant drugs should be expected to act on the DA system, especially by interfering with DA reuptake. Taking these findings into account, the DA system and its transmission might be of crucial importance for the comorbidity of drug use disorders in MDD [65].

Although drug use disorders have been studied for a long time, our understanding of its governing processes is still rather limited. One underlying mechanism seems to be the synaptic plasticity of neuronal pathways that are involved in reward and learning, and a corresponding hypothesis states that addictive drug use is a form of "pathological learning" [22,23,25]. Synaptic plasticity is the capability of a synapse to adjust its connection strength by changing the amount of released neurotransmitters and/or modifying the efficacy of its response to neurotransmitter stimulation [15]. The intensity of a response to neurotransmitters is determined by the density of postsynaptic receptors and by receptor conductance.

In this study, we focus on the DA system and the effects of DA transmission on synaptic plasticity, which is hypothesized as an underlying mechanism for addictive drug use. The nucleus accumbens (NAc) is selected as locus of interest because the mesolimbic DA pathway is critical to reward and addictive drug use [69]. NAc is located in the ventral striatum and receives inputs for basal ganglia, and it is a component of the important cortico-striato-pallido-thalamo-cortical loop. In addition to dopamine input, NAc also receives glutamate projections from the cortex that can affect effects of DA transmission on synaptic plasticity. The mechanisms for regulating synaptic plasticity involve both sides of a synapse, that is, the presynapse and the postsynapse. Metabolic processes in the presynapse determine the amount of released neurotransmitters through the control of enzymatic reactions and the recycling of neurotransmitter between different compartments. On the postsynaptic side, the density and conductance of receptors are regulated by second messenger systems and activity profiles of kinases and phosphatases. These regulatory mechanisms quantitatively and dynamically govern the resultant synaptic plasticity in a complex manner that exceeds the intuition of the human brain and necessitates support of a mathematical model. In the future, this model of synaptic plasticity in the comorbidity between drug use disorders and MDD will become even more complex when the roles of acetylcholine, serotonin and norepinephrine are merged with the present focus on dopamine.

Biochemical and Physiological Considerations

Nerve cells in NAc are mainly medium spiny neurons that receive several neurotransmitters, including dopamine and glutamate. Dopamine binds to its D_1 and D_2 receptors on the postsynaptic membranes of NAc neurons and activates or inhibits a second

messenger system (the cAMP system) which regulates the activity of protein kinase A (PKA) and the activity of protein phosphatase-1 (PP1). Glutamate binds to its ionotropic receptors (*e.g.*, AMPA and NMDA receptors) and regulates the calcium flux into the postsynapse. This calcium flux in turn regulates the activity of Ca^{2+}/calmodulin-dependent protein kinase (CaMKII) and the activity of protein phosphatase 2A (PP2A). These kinases and phosphatases control phosphorylation and dephosphorylation of AMPA receptors, and the density and conductance of these receptors are representations of the synaptic plasticity of GABAergic medium spiny neurons in the striatum (**Fig. 1b–c**).

Thus, the first component of the model addresses processes in the presynapse, which include neurotransmitter production, storage, recycling, and degradation. In the case of dopamine (DA), several processes and mechanisms are critical, namely: DA synthesis, catalyzed by the enzyme tyrosine hydroxylase (TH); the packaging of DA into vesicles through vesicular monoamine transporters (VMAT2); the degradation of DA by the enzyme monoamine oxidase (MAO); and the reuptake of DA by dopamine transporters (DAT). These processes are shown in **Fig. 2a**. The dynamics of glutamate is not modeled here. Instead, glutamate signals are simply represented by their main effect, which is the influx of calcium into the postsynapse.

The second component of the model addresses the postsynapse (**Fig. 2b**), where processes crucially important to the transduction of neurotransmitter signals include: the loop of PKA-phosphodiesterase (PDE)-cAMP-PKA (I, red line); interactions between different phosphorylation sites of DARPP-32 (the **d**opamine- and c**A**MP-**r**egulated **p**hospho**p**rotein with **32** kDa molecular weight); the positive feedback loop of PKA-PP2A-DARPP-32-PKA (II, green line); regulation of PKA and PP1 by different forms of DARPP-32 phosphorylation; the interaction between PP1 and CaMKII (III, lavender lines); and the interaction between PKA and PP1 via binding of Inhibitor-1 (I1) or via regulation of DARPP-32 phosphorylation (IV, blue lines). The details and magnitudes of the contributions of these component processes to synaptic plasticity are complicated and not yet entirely clear.

The third component of the model describes the phosphorylation, dephosphorylation and trafficking of AMPA receptors (AMPARs) in the postsynapse, which are regulated by the first and second model components presented above (**Fig. 2c**). AMPARs can be inserted into the membrane and removed from it based on their phosphorylation states, which are controlled by kinases and phosphatases. A buffer of AMPARs, controlled through synthesis and degradation, acts as a supply and storage unit for cytosolic AMPARs and communicates with the pool of membrane-associated AMPARs. Controlled by these mechanisms, membrane-associated AMPARs modify the synaptic efficacy of medium spiny neurons.

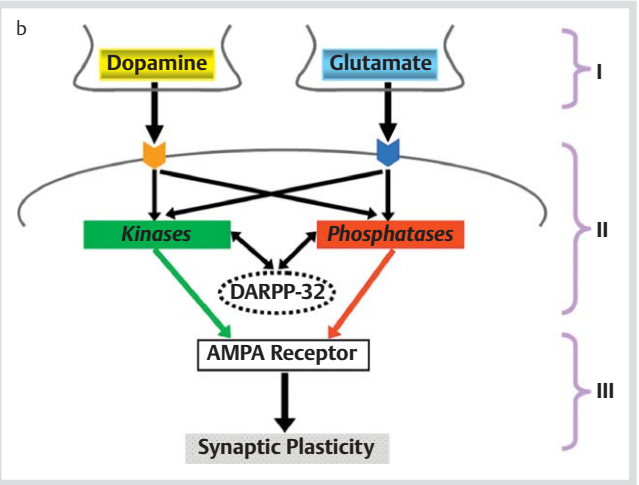

Fig. 1b The proposed computational model is structured in three modules, which are: I. neurotransmitter dynamics and release; II. signal transduction; III. trafficking of AMPA receptors. Each module is adapted from earlier work: a detailed model of dopamine metabolism similar to [48, 49]; a composite model of signal transduction based on [2, 14, 31, 50]; and a model of AMPAR dynamics adapted from [8, 18, 41].

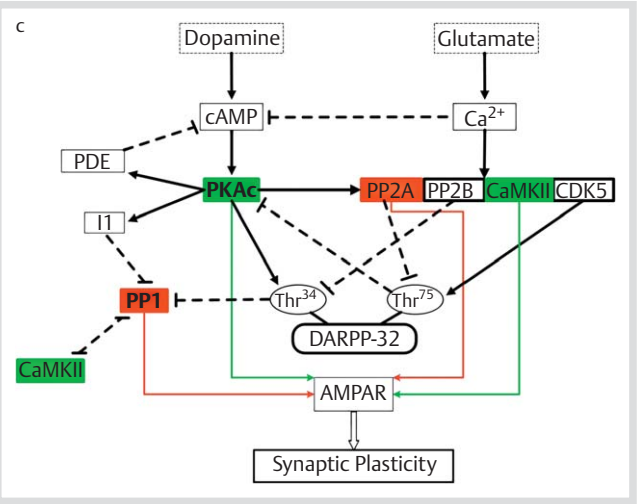

Fig. 1c Mechanisms within the postsynapse that integrate dopamine and glutamate signals from different presynaptic cells and ultimately lead to synaptic plasticity in neurons of the nucleus accumbens. Specifically, dopamine and glutamate signals affect the activity of various kinases and phosphatases, which interact with each other and with DARPP-32. Activity profiles of kinases and phosphatases regulate phosphorylation and dephosphorylation of AMPAR, whose density and conductance modify synaptic plasticity of GABAergic medium spiny neurons. Ovals attached to DARPP-32 and denoted as Thr^{34} and Thr^{75} indicate phosphate groups at two threonine residues; their numbers refer to positions in the rat sequence. Blunted lines represent inhibition signals. Green and red boxes are kinases and phosphatases, respectively.

Modeling Methods

The model is set up with ordinary differential equations (ODE) of biochemical reactions and signal transduction processes that describe the 3 components and ultimately connect dopamine and glutamate signals to synaptic plasticity of GABAergic medium spiny neurons. It is partially based on earlier models from our lab as well as from other groups. Specifically, the components of the system model include sub-modules for dopamine metabolism in the presynapse [48, 49], signal transduction in the postsynapse [2, 14, 31, 50], and trafficking of AMPA receptors [8, 18, 41] (**Fig. 1b**). These modules were adapted and integrated into a single model that accounts for signals of dopamine and glutamate, their transduction in medium spiny neurons, and their control of AMPA receptors, which are used as indicators of synaptic plasticity of medium spiny neurons in the striatum. In the following sections, we review the 3 component modules: (1) neurotransmitter dynamics and release, along with presynaptic effects of amphetamine; (2) signal transduction; (3) trafficking of

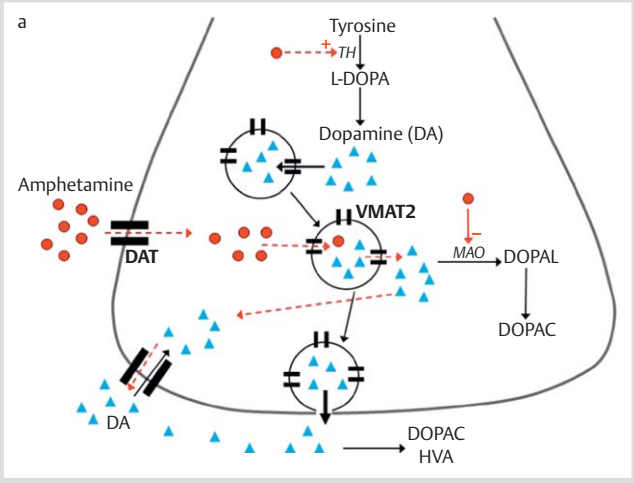

Fig. 2a Dopamine dynamics in the presynaptic terminal. Dopamine is synthesized from its precursor L-DOPA, which is produced from tyrosine. Most synthesized dopamine is packed into storage vesicles for later release into the synaptic cleft. Dopamine transporter (DAT) proteins can carry dopamine from the synaptic cleft back to the presynaptic terminal for recycling. In addition, dopamine can be enzymatically converted into other metabolites or diffuse out of the cleft. The psychostimulant amphetamine increases release of dopamine from the vesicles into the cytosol through vesicular monoamine transporters (VMAT2), and to the synaptic cleft via DAT. At the same time, amphetamine inhibits the enzyme monoamine oxidase (MAO), which degrades excess dopamine, and promotes synthesis of dopamine through activation of the enzyme tyrosine hydroxylase (TH). These mechanisms to alter dopamine metabolism in the presynapse by amphetamine are highlighted as red arrows.

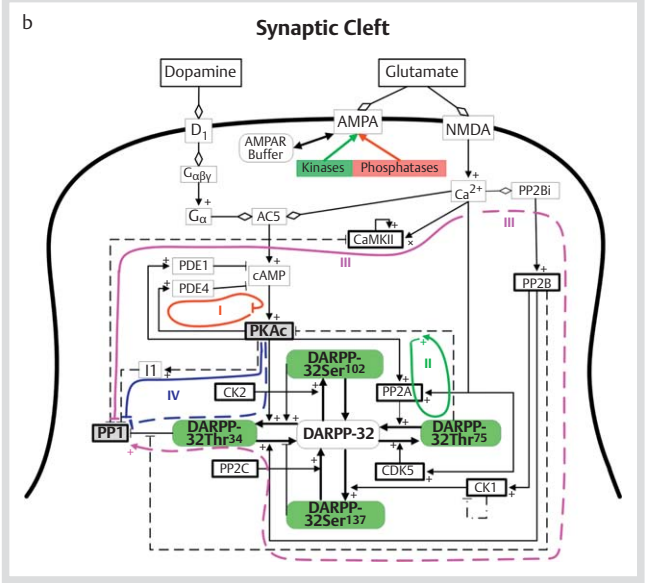

Fig. 2b Signal transduction in the postsynapse. Dopamine binds to its D_1 receptors and triggers the second-messenger cAMP, which subsequently activates protein kinase A (PKA). PKA phosphorylates DARPP-32 at a specific threonine residue and thereby converts it into a potent inhibitor of protein phosphatase-1 (PP1). In contrast, glutamate binds to its own receptors (AMPAR and NMDAR) and induces Ca^{2+} flux into the cell. The elevation of Ca^{2+} activates protein phosphatase 2B (PP2B), which dephosphorylates DARPP-32 and reduces its inhibition of PP1. Meanwhile, Ca^{2+} influx activates phosphorylation of DARPP-32 by cyclin-dependent kinase 5 (CDK5) at another threonine residue, which inhibits the activity of PKA. Color lines and dotted lines represent potentially critical mechanisms for synaptic plasticity and are subsystems under perturbation investigations: the negative feedback loop PKA – PDE – cAMP – PKA (I, the red line) ; the positive feedback loop of PKA – PP2A – DARPP-32-Thr75 – PKA (II, the green line); the alternative pathways of glutamate – PP2B – PP1 vs. glutamate – CaMKII – PP1 (III, the lavender lines); and alternative pathways of PKA – DARPP-32-Thr34 – PP1 vs. the pathway PKA – I1 – PP1 (IV, the blue lines).

AMPA receptors. Subsequently, we will discuss pertinent specifics of module integration and additional issues of model design.

Neurotransmitter dynamics and role of amphetamine: The neurotransmitter dopamine is synthesized from its precursor L-DOPA, which is produced from tyrosine (**Fig. 2a**). Most synthesized dopamine is packed into vesicles for storage and for later release into the synaptic cleft. Released dopamine can bind to its receptors on the postsynaptic membrane and transfer neuronal signals. As an alternative to receptor binding, dopamine transporter (DAT) can carry the released dopamine back into the presynaptic terminal for recycling. Within the terminal and the synaptic cleft, dopamine can be enzymatically converted into other metabolites. The dopamine signal leaving the presynapse is composed of a basal level and the stimulated release in response to electrical signals received by the presynaptic membrane. The psychostimulant amphetamine increases the release of dopamine from vesicles into the cytosol through VMAT2 and to the synaptic cleft via DAT [66]. At the same time, it inhibits the enzyme MAO, which degrades excess dopamine, and promotes synthesis of dopamine through activation of the enzyme tyrosine hydroxylase (TH) [66]. Glutamate is produced and degraded in different neurons and glia cells. For simplicity, glutamate signals are represented here by their main effect, namely the influx of calcium into the postsynapse.

Signal transduction: In the presence of dopamine, the D_1 receptors are activated while the D_2 receptors are inhibited. Since the D_1 and D_2 receptors regulate cAMP antagonistically, the effects of D_2 receptors in response to dopamine stimulation can be represented indirectly and in first approximation through the function of D_1. Because mechanistic details of the antagonistic action are not known quantitatively, and in order to keep our model as simple as feasible, we therefore include only dopamine D_1 receptors in our model. When dopamine binds to its postsynaptic receptors of D_1 subtype, a G-protein based mechanism triggers a second-messenger cAMP system (**Fig. 2b**). The cAMP system in turn activates protein kinase A (PKA). PKA then phosphorylates DARPP-32 at a specific threonine residue (DARPP-32-Thr34, where 34 refers to the position in the rat sequence) and thereby converts it into a potent inhibitor of protein phosphatase-1 (PP1).

Glutamate binds to its own ionotropic receptors (*e.g.*, AMPAR and NMDAR) and induces Ca^{2+} flux into the cell. The elevation of Ca^{2+} activates protein phosphatase 2B (PP2B), which dephosphorylates DARPP-32 and reduces its inhibition of PP1. Meanwhile, Ca^{2+} influx activates phosphorylation of DARPP-32 by cyclin-dependent kinase 5 (CDK5) at another threonine residue (DARPP-32-Thr75), which inhibits the activity of PKA.

Trafficking of AMPA receptors: In response to dopamine and glutamate signals and their effects on DARPP-32, the kinases and phosphatases affect the phosphorylation and dephosphorylation state of AMPARs and thus their membrane insertion or removal, which in turn modifies the synaptic efficacy of medium spiny

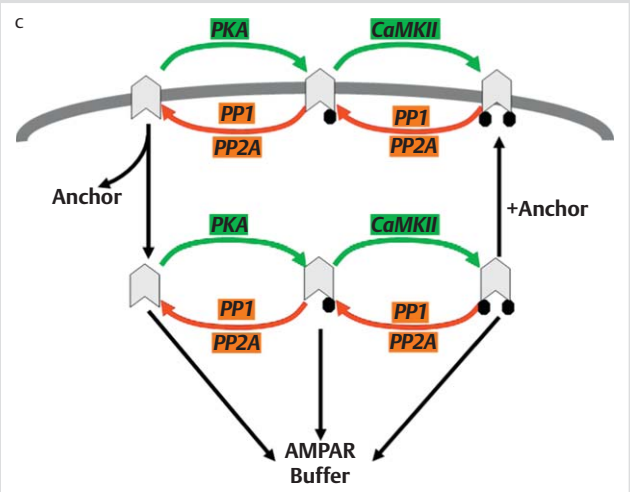

Fig. 2c Trafficking of AMPA receptors (AMPARs) in the postsynapse. In response to dopamine and glutamate signals that reach DARPP-32, kinases and phosphatases in the postsynapse affect membrane insertion and removal of AMPARs, which modify the synaptic efficacy of medium spiny neurons. The kinase PKA can phosphorylate AMPARs at site Ser845, while another kinase CaMKII can phosphorylate site Ser831. Both sites can be dephosphorylated by phosphatases PP1 and PP2A. The double phosphorylation of cytosolic AMPARs enables the insertion of AMPARs into the membrane. Unphosphorylated AMPARs can move back to cytosol. In addition, an AMPAR buffer supplies or stores cytosolic AMPARs as needed. Thus, AMPARs move between membrane, cytosol, and the storage buffer.
Abbreviations: 3-4-dihydroxy-phenylacetaldehyde (DOPAL), homovanillate (HVA), 3,4-dihydroxyphenylacetate (DOPAC), cyclic AMP (cAMP), NMDA receptor (NMDAR), AMPA receptor (AMPAR), protein phosphatase 2A (PP2A), dopamine- and cAMP-regulated phosphoprotein with 32 kDa molecular weight (DARPP-32), Ca^{2+}/calmodulin-dependent protein kinase (CaMKII), cytosolic AMPAR (cAMPAR), membrane-associated AMPAR (mAMPAR), buffered AMPAR (bulk_cAMPAR).

neurons (**Fig. 2c**). The kinase PKA can phosphorylate AMPAR at site Ser845, while another kinase CaMKII can phosphorylate site Ser831. Both sites can be dephosphorylated by the phosphatase PP1 and the protein phosphatase PP2A. The double phosphorylation of AMPAR enables the binding of an anchor and the insertion of cytosolic AMPAR into the postsynaptic membrane. The unphosphorylated form of AMPAR separates from the anchor and moves back into the cytosol. A buffer of AMPARs, which is controlled by their synthesis and degradation, acts as a supply and deposit of cytosolic AMPAR. Thus, AMPARs travel between membrane, cytosol, and the buffer in different phosphorylation states.

Model equations: The integrative model for synaptic plasticity of GABAergic medium spiny neurons in the striatum is set up based on ODEs and the law of mass action. Specifically, all reactions are represented in the form of an enzymatic reaction (Eq. 1) or a simple binding reaction (Eq. 2):

$$S + E \underset{K_b}{\overset{K_f}{\rightleftharpoons}} SE \xrightarrow{K_c} P + E \qquad \text{(Eq. 1)}$$

$$A + B \underset{K_b}{\overset{K_f}{\rightleftharpoons}} AB \qquad \text{(Eq. 2)}$$

Features regarding dopamine metabolism in the presynapse were taken directly from [48] and are not repeated here. The remaining reactions and their kinetic details are listed in **Table 1–3** in the appendix. Initial conditions for the differential equations are presented in **Table 4**. Altogether, the integrated model consists of 121 ordinary differential equations. After typical diagnostics of stability and robustness (*e.g.*, [71,72]), which showed that the model behaves properly, we simulated the responses of the system to various dopamine and glutamate signals and in the context of comorbid drug use in MDD. These simulations included different scenarios of neurotransmitter depletion, low frequency stimulation (LFS), and high frequency stimulation (HFS). Dopamine and glutamate signals were considered separately as well as in combination. Subsequently, drug injection of the psychostimulant amphetamine was simulated. Finally, we perturbed mechanisms that have the potential of critically affecting synaptic plasticity and observed their effects on the performance of the system in response to various input signals.

Results

Synaptic plasticity caused by dopamine and glutamate

A necessary step between model construction and application is the testing and validation of the model against biological and clinical observations. In the current context, these observations consist primarily of electrophysiological data. Specifically, the following observations of changes in synaptic efficacy in response to different stimuli of dopamine and glutamate are important.

1. **Corticostriatal HFS → Synaptic depression:** Corticostriatal high-frequency stimulation causes the release of glutamate and induces reduction of synaptic efficacy of the GABAergic medium spiny neurons. This reduction is termed *synaptic depression* [6,7,74].
2. **Corticostriatal HFS/substantia nigra HFS → Synaptic potentiation:** Simultaneous high-frequency stimulation of projections from the cortex and the substantia nigra (or the ventral tegmental area), which release both glutamate and dopamine, results in an elevation of the synaptic efficacy of GABAergic medium spiny neurons. This phenomenon is known as *synaptic potentiation* [55,57,74].
3. **Corticostriatal HFS/DA depletion → No change in efficacy or synaptic depression:** When rat brain slices are stimulated through corticostriatal high-frequency stimulation and simultaneously depleted of striatal dopamine by toxic 6-hydroxydopamine, the change in synaptic efficacy is either undetectable or tends toward synaptic depression of the GABAergic medium spiny neurons [57,68].
4. **Substantia nigra HFS → Synaptic potentiation:** High-frequency stimulation of the substantia nigra (or the ventral tegmental area) causes the release of dopamine and induces elevated synaptic efficacy in GABAergic medium spiny neurons [55].
5. **Corticostriatal HFS/AMPT → Synaptic depression:** Reduction of dopamine release in the striatum through pretreatment with α-methyl paratyrosine (AMPT) does not block the synaptic depression induced by corticostriatal HFS [57].
6. **Corticostriatal HFS/substantia nigra LFS → Synaptic potentiation:** Low-frequency stimulation of the substantia nigra (or the ventral tegmental area) blocks synaptic depression from corticostriatal HFS and induces a short period of synaptic potentiation [56].

We simulated all these different signal scenarios and compared simulated results with electrophysiological observations. In these simulations, the basal levels of dopamine and calcium cation were set to 10 nM and 50 nM, respectively. The stimulated

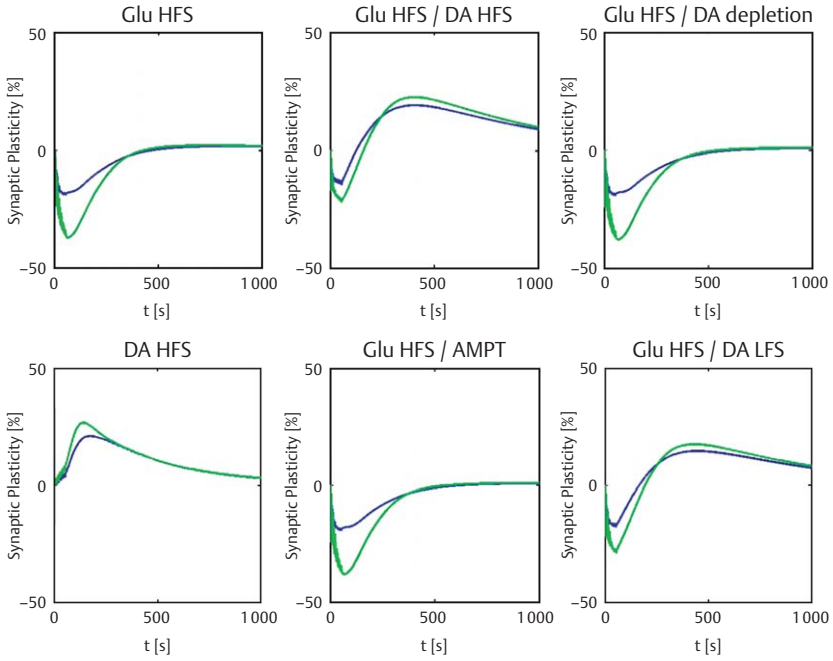

Fig. 3 Typical synaptic plasticity of GABAergic medium spiny neurons in response to various stimuli to the corticostriatal projections and the substantia nigra (or the ventral tegmental area). Time is given in units of seconds, while synaptic plasticity is expressed as the ratio of the number of membrane-associated AMPARs after and before a stimulus (blue lines), and as ratio of conductance of membrane-associated AMPARs (green lines).

dopamine level maximally reached 2 µM, while activated calcium cation maximally reached 5 µM. Synaptic plasticity was represented by the ratio of the number of membrane AMPARs after and before a particular stimulus. In consideration of the conductance difference between different phosphorylated forms of membrane AMPARs, we used a formula to calibrate the computation of synaptic plasticity. In this formula, single phosphorylation raises the basal conductance by 50%, while double phosphorylation is assumed to result in twofold basal conductance. Overall, the results of the model simulations demonstrated good consistency with electrophysiological observations (**Fig. 3**).

The model simulations identified 2 interesting phenomena of potential importance. First, they showed that changes in synaptic plasticity are mostly of short duration, with a typical time frame of about 10 min. This result is consistent with the observation that synaptic potentiation caused by substantia nigra (or the ventral tegmental area) stimulation mostly lasts for 10–15 min [56]. The second interesting result is a temporary synaptic depression, which precedes synaptic potentiation in cases of concurrent dopamine and glutamate signals. We are not aware of clinical observations of this effect.

Synaptic plasticity caused by amphetamine and comorbidity with MDD

To study the effect of the psychostimulant amphetamine on synaptic plasticity of GABAergic medium spiny neurons, we incorporated the mechanisms triggered by amphetamine into the model of dopamine metabolism and compared its output with experimental observations [78]. A comparison of results showed that the model produced dynamic responses of extracellular dopamine very similar to those measured by the brain dialysis (results not shown).

Accounting for the effects of amphetamine in the model, we also simulated effects of different amounts of amphetamine on synaptic plasticity of GABAergic medium spiny neurons, with dosages varying from 0.1 mg/kg to 5 mg/kg, a range that corresponds to street use and medical treatments. The effective period of 0.5 mg/kg amphetamine turned out to be longer than 2 h, thus requiring an increased time window for the simulations. As the results show, a single injection of 0.5 mg/kg amphetamine can potentiate synaptic efficacy to a level that corresponds to about 3 times the basal level (**Fig. 4a, b**). The system behaves quasi in a bistable way, and the synaptic potentiation lasts for over 2 h.

As there is suspected comorbidity between drug use disorders and MDD, we also studied the effect of the psychostimulant amphetamine on synaptic plasticity within an MDD-impaired DA system. Since antidepressants block the reuptake of monoamines, we simulated the opposite of this process in order to reflect MDD, namely an increased (doubled) activation of DAT. We then challenged the impaired system with a single injection of 0.5 mg/kg amphetamine (**Fig. 4c, d**). The results show that activation of DA reuptake impairs DA transmission and causes a reduced reward of amphetamine in MDD. Furthermore, the impairment of DA transmission leads to a reduced synaptic potentiation effect of the psychostimulant. Another intervention causing reduced reward is the application of dopamine D_1 antagonists (e.g., SCH 39166), which in a model simulation causes an alteration of amphetamine effects on synaptic plasticity (data not shown).

Effects of various mechanisms on synaptic plasticity

In an additional set of simulations of a different type, we perturbed mechanisms in the system that we expected to be potentially important to synaptic plasticity of GABAergic medium spiny neurons. These prescreened mechanisms included: the negative feedback loop PKA – PDE – cAMP – PKA (I, **Fig. 2b**); the positive feedback loop of PKA – PP2A – DARPP-32-Thr75 – PKA (II, **Fig. 2b**); differences in responses of the pathway of glutamate – PP2B – PP1 *vs.* glutamate – CaMKII – PP1 (III, **Fig. 2b**); and differences in responses of the pathway PKA – DARPP-32-Thr34 – PP1 *vs.* the PKA – I1 – PP1 (IV, **Fig. 2b**). Besides these mechanisms in the postsynapse, we tested processes in the presynapse that were identified as particularly critical in the context of psychostimulants. Specifically, it has been suggested that amphetamine affects the synthesis, storage, recycling, and degradation of dopamine (red arrows in **Fig. 2a**). These processes are primarily related to the function of VMAT2,

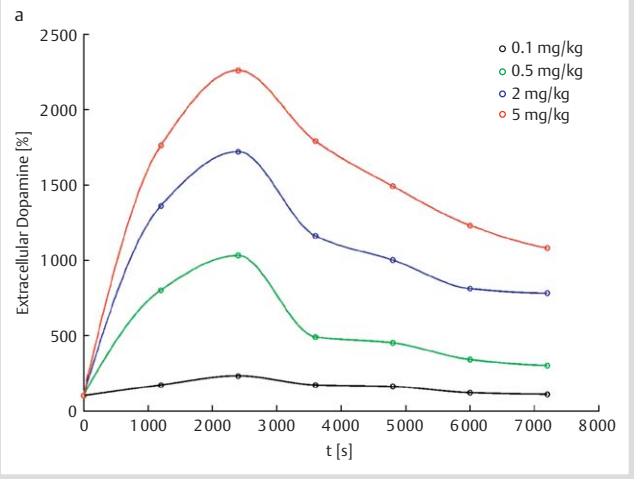

Fig. 4a Effect of amphetamine on the synaptic plasticity of GABAergic medium spiny neurons. Experimental measurements (connected symbols) of released dopamine following single injections of different doses of amphetamine, namely 0.1 mg/kg, 0.5 mg/kg, 2.0 mg/kg, and 5.0 mg/kg.

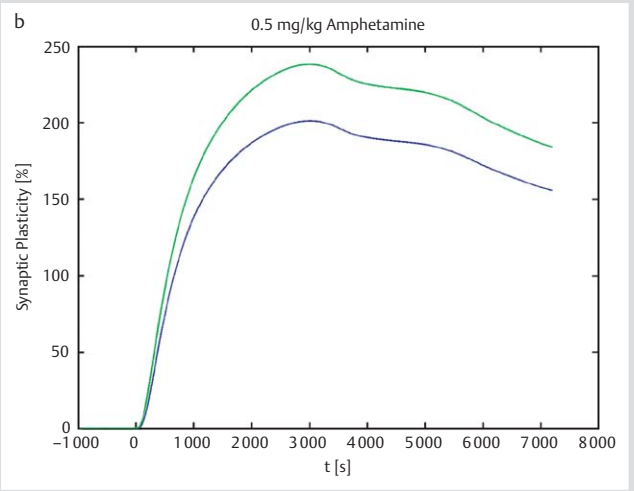

Fig. 4b Effect of amphetamine on the synaptic plasticity of GABAergic medium spiny neurons. Synaptic plasticity caused by a single dose of 0.5 mg/kg amphetamine. Blue line: ratio of membrane-associated AMPARs after and before the injection of amphetamine. Green line: ratio of conductance of membrane-associated AMPARs after and before the injection of amphetamine.

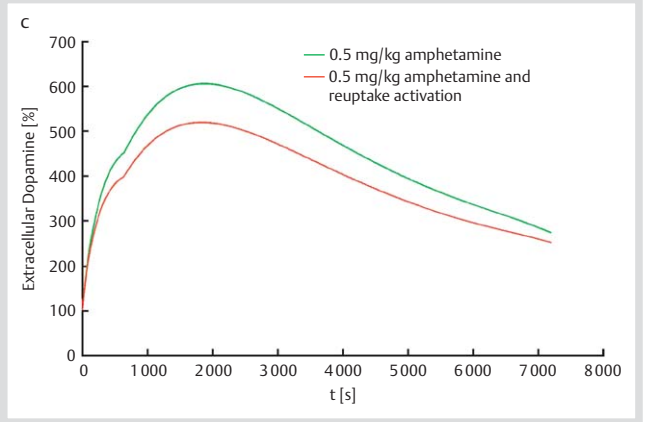

Fig. 4c Effect of amphetamine on the synaptic plasticity of GABAergic medium spiny neurons. Activation of DA reuptake, as it is presumably found in MDD, impairs DA transmission and causes a reduced reward for the consumption of amphetamine. Green line: DA released by a single dose of 0.5 mg/kg amphetamine in a normal DA system. Red line: DA released by a single dose of 0.5 mg/kg amphetamine in a DA system with activation of DA reuptake.

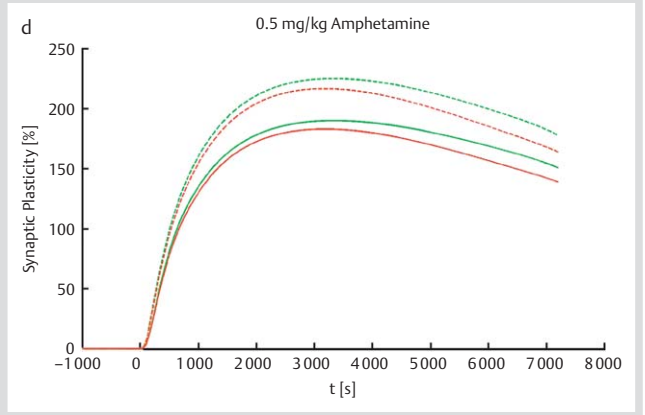

Fig. 4d Effect of amphetamine on the synaptic plasticity of GABAergic medium spiny neurons. The impairment of DA transmission by reuptake activation in the case of MDD leads to a reduced synaptic potentiation effect of the psychostimulant amphetamine. Solid lines: ratios of the number of membrane-associated AMPARs after and before a stimulus. Dashed lines: ratios of conductance of membrane-associated AMPARs after and before a stimulus. Green lines represent the normal DA system. Red lines represent the DA system with MDD-induced activation of DA reuptake.

DAT, MAO-B, and catechol O-methyltransferase (COMT). Therefore, we perturbed these components before applying amphetamine and studied their effects on synaptic plasticity. Perturbations of the involved mechanisms consisted of 10-fold activation and inhibition, which were implemented per multiplication of the relevant rate constants by 10 or 0.1, respectively.

(I) PKA – PDE – cAMP – PKA: This negative feedback loop is in effect because PKA phosphorylates PDE, both PDE and its phosphorylated form convert cAMP into AMP, and cAMP activates PKA (**Fig. 5a**). Simulations show that perturbations of this negative loop have a negligible influence on glutamate signals. However, this loop is critical to dopamine signals. Inhibition of this module eliminates the effects of dopamine on synaptic plasticity. Under this inhibition, even substantia nigra HFS (or the ventral tegmental area HFS) cannot induce synaptic potentiation. For concurrent signals of corticostriatal HFS/substantia nigra LFS, inhibition of this pathway causes synaptic depression instead of synaptic potentiation when there is no perturbation or an activation of the PKA – PDE – cAMP – PKA loop is applied (**Fig. 5b**).

(II) PKA – PP2A – DARPP-32-Thr75 – PKA: PKA activates PP2A, which is the phosphatase responsible for removal of the phosphate at threonine residue 75 of DARPP-32. Since DARPP-32 phosphorylated at Thr75 inhibits PKA, these processes together form a positive feedback loop (**Fig. 6a**). The simulation results show that inhibition of this positive feedback loop can counteract the synaptic depression effect of glutamate signals (**Fig. 6b**). For dopamine signals, however, activation of this loop enhances synaptic potentiation. In response to concurrent dopamine and glutamate signals, inhibition of this loop – rather than its activation – counteracts the synaptic depression effect of glutamate signals.

Quantitatively, this positive feedback loop contributes more significantly to the effects of dopamine rather than glutamate.

(III) Glutamate – PP2B – PP1 vs. Glutamate – CaMKII – PP1: Glutamate activates phosphatase PP2B, which removes phosphate at Thr34 residue of DARPP-32. Because this dephosphorylation releases DARPP-32 inhibition of PP1, glutamate activates PP1 through this pathway. However, the autophosphorylation of the kinase CaMKII is also activated by glutamate and then inhibits PP1. Therefore, the effect of glutamate on synaptic plasticity can vary, depending on the relative magnitudes of its activation and its inhibition of PP1 (**Fig. 7a**). Inhibition of PP1 can be obtained through activation of the glutamate – CaMKII – PP1 pathway, which shows enhanced effects of both dopamine and glutamate signals. By contrast, inhibition of the glutamate – CaMKII – PP1 pathway diminishes the normal effects of both dopamine and glutamate signals so that corticostriatal HFS induces synaptic potentiation instead of synaptic depression (**Fig. 7b**). In contrast to the glutamate – CaMKII – PP1 pathway, the glutamate – PP2B – PP1 pathway has a less significant impact on synaptic plasticity.

(IV) PKA – DARPP-32-Thr34 – PP1 vs. PKA – I1 – PP1: PKA indirectly inhibits PP1 through 2 pathways: one is PKA – DARPP-32-Thr34 – PP1 and the other is PKA – I1 – PP1 (**Fig. 8a**). It is interesting to investigate their relative significance for the regulation of synaptic plasticity. Our simulations show that PKA inhibition of PP1 through DARPP-32-Thr34 is more effective than inhibition through the PKA – I1 – PP1 pathway (**Fig. 8b**). Increased PKA inhibition of PP1 potentiates dopamine-induced synaptic plasticity, while reduced inhibition of PP1 by PKA diminishes dopamine-induced synaptic potentiation.

Perturbations affecting VMAT2, DAT, MAO-B, or COMT: A perturbation affecting each of these molecules was applied before a single application of 0.5 mg/kg amphetamine. Our simulations showed that the enzymes MAO-B and COMT are less significant than the transporters VMAT2 and DAT with respect to amphetamine effects on synaptic plasticity. Activation of DAT diminishes synaptic potentiation caused by amphetamine, while DAT inhibition enhances it (results not shown).

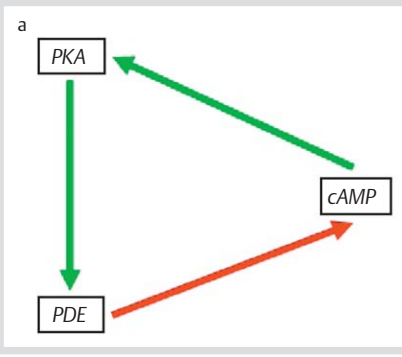

Fig. 5a Effect of the negative feedback loop PKA – PDE – cAMP – PKA on synaptic plasticity of GABAergic medium spiny neurons. Functional diagram of the loop PKA – PDE – cAMP – PKA. Green arrow: activation; red arrow: inhibition.

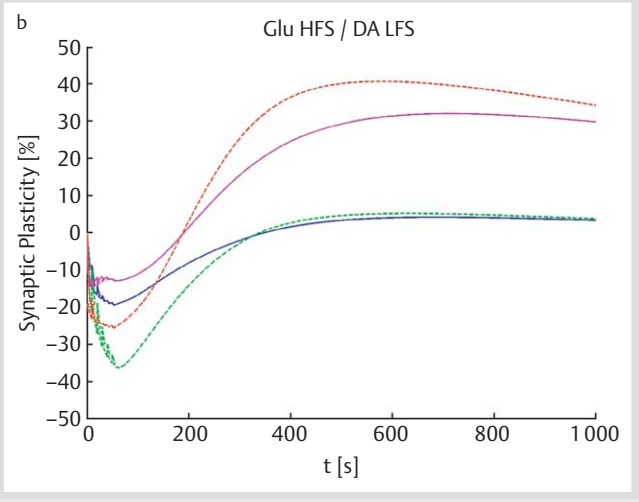

Fig. 5b Effect of the negative feedback loop PKA – PDE – cAMP – PKA on synaptic plasticity of GABAergic medium spiny neurons. High-frequency stimulation of the corticostriatal projections (Glu HFS), together with high-frequency stimulation of the substantia nigra or the ventral tegmental area (DA HFS). Solid lines: ratios of membrane-associated AMPARs after and before a stimulus. Dashed lines: ratios of conductance of membrane-associated AMPAR after and before a stimulus. Blue and green lines represent inhibition of the loop. Magenta and red lines represent activation of the loop.

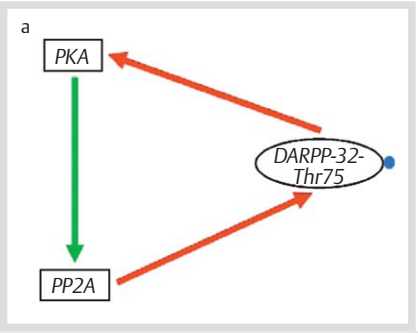

Fig. 6a Effect of the positive feedback loop PKA – PP2A – DARPP-32-Thr75 – PKA on the synaptic plasticity of GABAergic medium spiny neurons. Functional diagram of the positive feedback loop PKA – PP2A – DARPP-32-Thr75 – PKA. Green arrows: activation; red arrows: inhibition. The blue hexagon attached to DARPP-32 indicates the phosphate group at Thr75.

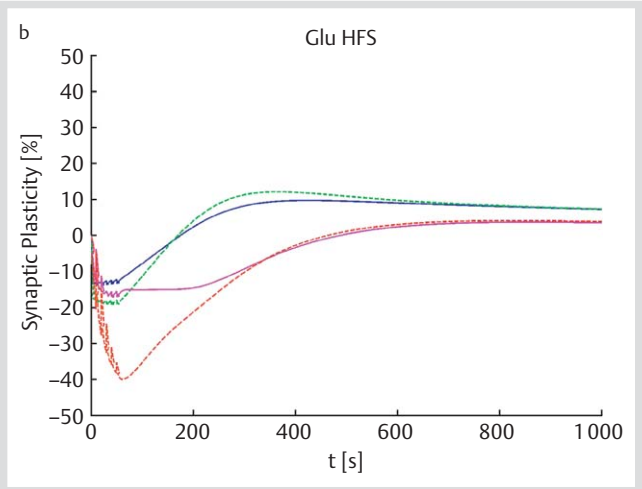

Fig. 6b Effect of the positive feedback loop PKA – PP2A – DARPP-32-Thr75 – PKA on the synaptic plasticity of GABAergic medium spiny neurons. High-frequency stimulation of the corticostriatal projections (Glu HFS). Solid lines: ratios of the number of membrane-associated AMPARs after and before a stimulus. Dashed lines: ratios of conductance of membrane-associated AMPARs after and before a stimulus. Blue and green lines represent inhibition of the loop. Magenta and red lines represent activation of the loop.

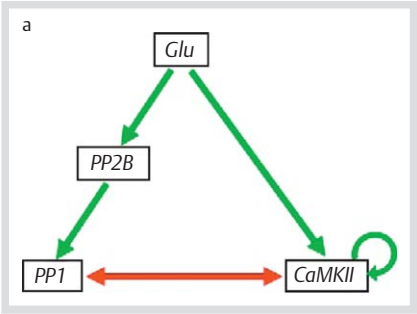

Fig. 7a Regulation of PP1 by glutamate through CaMKII has a more significant effect on the synaptic plasticity of GABAergic medium spiny neurons than regulation of PP1 through PP2B. Functional diagram of the regulation of PP1 by glutamate through PP2B and CaMKII. Green arrow: activation; red arrow: inhibition.

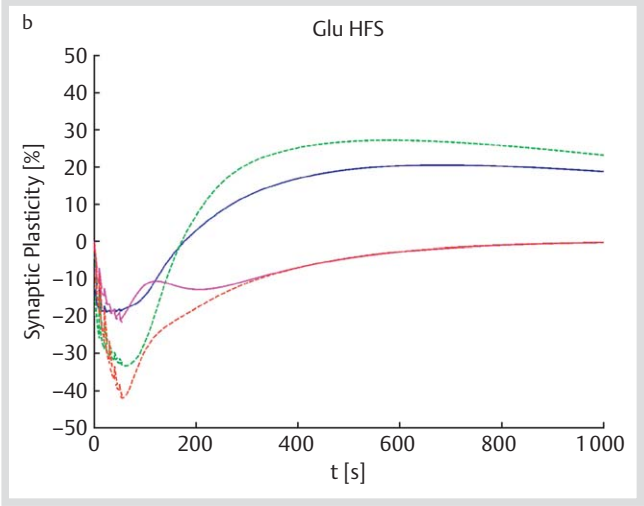

Fig. 7b Regulation of PP1 by glutamate through CaMKII has a more significant effect on the synaptic plasticity of GABAergic medium spiny neurons than regulation of PP1 through PP2B. High-frequency stimulation of the substantia nigra or the ventral tegmental area (DA HFS). Solid lines: ratios of membrane-associated AMPARs after and before a stimulus. Dashed lines: ratios of conductance of membrane-associated AMPAR after and before a stimulus. Blue and green lines represent inhibition of the pathway Glutamate – CaMKII – PP1. Magenta and red lines represent activation of this pathway.

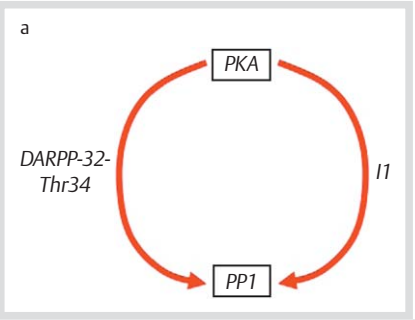

Fig. 8a Inhibition of PP1 by PKA through DARPP-32 has a more significant effect on the synaptic plasticity of GABAergic medium spiny neurons than inhibition of PP1 through I1. Functional diagram of the inhibition of PP1 by PKA through DARPP-32-Thr34 and I1. Green arrow: activation; red arrow: inhibition.

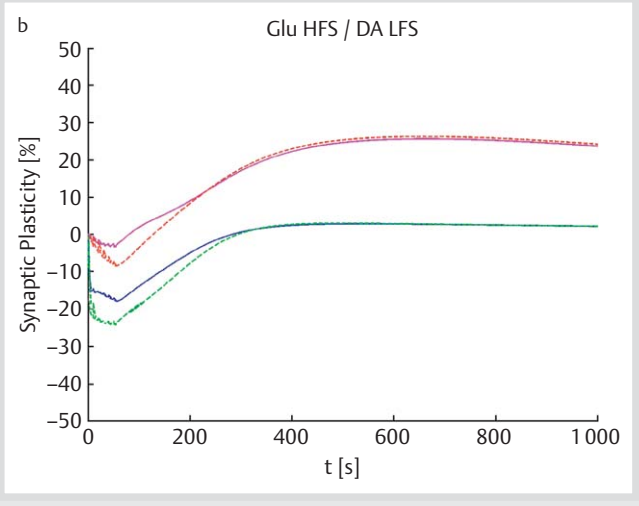

Fig. 8b Inhibition of PP1 by PKA through DARPP-32 has a more significant effect on the synaptic plasticity of GABAergic medium spiny neurons than inhibition of PP1 through I1. High-frequency stimulation of the corticostriatal projections (Glu HFS), together with high-frequency stimulation of the substantia nigra or the ventral tegmental area (DA HFS). Solid lines: ratios of membrane-associated AMPARs after and before a stimulus. Dashed lines: ratios of conductance of membrane-associated AMPARs after and before a stimulus. Blue and green lines represent inhibition of the pathway PKA – DARPP-32-Thr34 – PP1. Magenta and red lines represent activation of this pathway.

Conclusions and Discussion

MDD patients have a strongly elevated risk of developing comorbidity with drug use disorders. Aggravating the situation, the model presented here suggests that the reward from drug use decreases in MDD-impaired DA systems, which will likely lead to the consumption of even higher doses of psychostimulants. Without treatment, the relapse rate among drug abusers within one year is as high as 90% [29]. One reason for this unfortunate situation may be an insufficient understanding of their underlying mechanisms. It has been suggested that synaptic plasticity might be one of such mechanisms. Therefore, it is important to characterize synaptic plasticity in detail. Specifically, it seems useful to screen and manipulate those mechanisms that are potentially critical to synaptic plasticity and to explore means of altering and correcting drug-caused modifications. Of course it is difficult to study alterations and manipulations of the reward system in a systematic fashion *in situ*, and the reward system itself is too complicated to use intuition as the sole means of explanation. By contrast, a computational model of the system, once constructed and validated, is easily simulated, manipulated with precisely targeted interventions and optimized toward a desirable goal. In this paper, we present how such an analysis can be performed.

Two molecular mechanisms are primarily utilized for synaptic plasticity: (1) modification of existing proteins; and (2) regulation of gene transcription and translation into new protein [54, 62]. The second mechanism accounts for long-lasting effects, but requires a longer response time than the first mechanism does, because gene expression is a much slower process than metabolic regulation and protein degradation.

In this study, we focused on the short-term effects of 2 neurotransmitters, dopamine and glutamate, and on alterations of their effects under drug abuse. Under normal conditions, dopamine and glutamate effects last for about 10–20 min, but this time period extends to over 2 h under the influence of

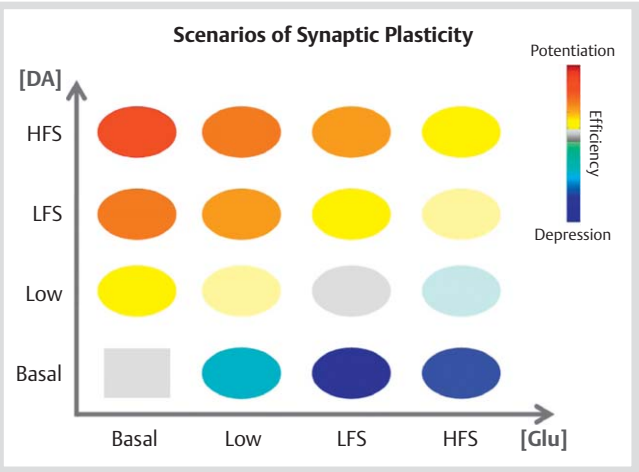

Fig. 9 Synaptic plasticity of GABAergic medium spiny neurons in response to various stimuli. The synaptic plasticity of GABAergic medium spiny neurons depends on the various combinations of concurrent stimuli of corticostriatal projections and substantia nigra (or the ventral tegmental area). LFS: low frequency stimulation; HFS: high frequency stimulation. Grey areas reflect negligible effects.

amphetamine. Glutamate signals are released by neurons projected from the cortex to the striatum, while dopamine signals come from striatal projections of dopaminergic neurons. In the striatum, the GABAergic medium spiny neurons typically respond to dopamine stimuli with synaptic potentiation and to glutamate signals with synaptic depression. Under concurrent dopamine and glutamate signals, the synaptic plasticity varies with input combinations (**Fig. 9**). Interestingly, a single dose of 0.5 mg/kg amphetamine makes synaptic plasticity of medium spiny neurons behave like a quasi-bistable system.

The effects of dopamine and glutamate signals on synaptic plasticity depend on several important processes. The positive feedback loop of PKA – PP2A – DARPP-32-Thr75 – PKA is important for effects of dopamine on synaptic plasticity. The negative feedback loop of PKA – PDE – cAMP – PKA is also critical with respect to dopamine, because inhibition of this module eliminates responses of the system to dopamine. Drug abuse commonly causes dopamine release in the NAc, and behavioral observations indicate that the mesolimbic dopamine pathway is directly involved in drug rewards [12]. As a consequence, these 2 feedback loops should be further investigated, because their alteration might have the potential of reversing drug use disorders. The glutamate signal from the cortex is similarly critical for drug-induced adaptations of neuronal behavior. Our results suggest that glutamate relies more on the glutamate – CaMKII – PP1 pathway than on the glutamate – PP2B – PP1 mechanism with respect to the regulation of synaptic plasticity. Dopamine and glutamate signals interact with each other through multiple pathways. One of these pathways is the inhibition of PP1 by PKA. The model simulations indicate that the indirect inhibition of PP1 through DARPP-32-Thr34 might actually be more effective than the inhibition of PP1 through I1.

Our current study focuses on short-term plasticity, which is important for early responses to drug exposures as well as the induction of long-term adaptations. However, drug use disorders are not formed immediately after an initial drug abuse. It requires chronic drug abuse and its time frame might range from weeks to months to years. These time scales most likely allow additional, significant contributions to synaptic plasticity from altered gene transcription and protein translation, as described above. One of the relevant molecules which control gene expression in this context is the transcription factor CREB (cAMP responsive element-binding protein), which, like some other components of long-term responses, will be analyzed in future work.

The mathematical model of synaptic plasticity of GABAergic medium spiny neurons that we presented here permits targeted manipulations and unlimited explorations of what-if scenarios. In particular, it allows comparative analyses between normal responses and responses under the influence of psychostimulants, in the absence or presence of MDD-induced impairments of the DA system. As we have shown, such analyses can characterize the relative importance of different components, such as the various control loops within the system. Since reward mechanisms activated by psychostimulants could be crucial in establishing addictive comorbidity in patients with MDD, this model might become an aid for targeting specific processes and modules within the reward system and lead to a better understanding and potential treatment of the comorbidity between drug use disorders and MDD.

Acknowledgements

This work was supported by a grant from the National Institutes of Health (P01-ES016731, Gary W. Miller, PI) and a grant from the University System of Georgia (EOV, PI). Any opinions, findings, and conclusions or recommendations expressed in this material are those of the authors and do not necessarily reflect the views of the sponsoring institutions. Felix Tretter obtained no financial support for his contribution.

Conflict of Interests

With regard to the present paper the authors have no conflicts of financial interests.

References

1 *APA*. Diagnostic and Statistical Manual of Mental Disorders (DSM-IV-TR Fourth Edition; Text Revision). Washington, DC: Americal Psychiatric Association; 2000
2 *Barbano PE*, *Spivak M*, *Flajolet M et al*. A mathematical tool for exploring the dynamics of biological networks. Proc Natl Acad Sci USA 2007; 104: 19169–19174
3 *Bewernick BH*, *Hurlemann R*, *Matusch A et al*. Nucleus accumbens deep brain stimulation decreases ratings of depression and anxiety in treatment-resistant depression. Biol Psychiatry 2010; 67: 110–116
4 *Bhalla US*, *Iyengar R*. Emergent properties of networks of biological signaling pathways. Science 1999; 283: 381–387
5 *Bibb JA*, *Snyder GL*, *Nishi A et al*. Phosphorylation of DARPP-32 by Cdk5 modulates dopamine signalling in neurons. Nature 1999; 402: 669–671
6 *Calabresi P*, *Centonze D*, *Gubellini P et al*. Glutamate-triggered events inducing corticostriatal long-term depression. J Neurosci 1999; 19: 6102–6110
7 *Calabresi P*, *Pisani A*, *Mercuri NB et al*. Long-term Potentiation in the Striatum is Unmasked by Removing the Voltage-dependent Magnesium Block of NMDA Receptor Channels. Eur J Neurosci 1992; 4: 929–935
8 *Castellani GC*, *Bazzani A*, *Cooper LN*. Toward a microscopic model of bidirectional synaptic plasticity. Proc Natl Acad Sci USA 2009; 106: 14091–14095
9 *Conner KR*, *Pinquart M*, *Holbrook AP*. Meta-analysis of depression and substance use and impairment among cocaine users. Drug Alcohol Depend 2008; 98: 13–23
10 *Dackis CA*, *Gold MS*, *Sweeney DR*. The physiology of cocaine craving and 'crashing'. Arch Gen Psychiatry 1987; 44: 298–300
11 *Desdouits F*, *Cheetham JJ*, *Huang HB et al*. Mechanism of inhibition of protein phosphatase 1 by DARPP-32: studies with recombinant DARPP-32 and synthetic peptides. Biochem Biophys Res Commun 1995; 206: 652–658

12 *Di Chiara G*, *Imperato A*. Drugs abused by humans preferentially increase synaptic dopamine concentrations in the mesolimbic system of freely moving rats. Proc Natl Acad Sci USA 1988; 85: 5274–5278
13 *Drevets WC*, *Price JL*, *Furey ML*. Brain structural and functional abnormalities in mood disorders: implications for neurocircuitry models of depression. Brain Struct Funct 2008; 213: 93–118
14 *Fernandez É*, *Schiappa R*, *Girault JA et al*. DARPP-32 is a robust integrator of dopamine and glutamate signals. PLoS Comput Biol 2006; 2: e176
15 *Gaiarsa JL*, *Caillard O*, *Ben-Ari Y*. Long-term plasticity at GABAergic and glycinergic synapses: mechanisms and functional significance. Trends Neurosci 2002; 25: 564–570
16 *Gawin FH*, *Kleber HD*. Abstinence symptomatology and psychiatric diagnosis in cocaine abusers. Clinical observations. Arch Gen Psychiatry 1986; 43: 107–113
17 *Girault JA*, *Hemmings HC Jr*, *Williams KR et al*. Phosphorylation of DARPP-32, a dopamine- and cAMP-regulated phosphoprotein, by casein kinase II. J Biol Chem 1989; 264: 21748–21759
18 *Hayer A*, *Bhalla US*. Molecular switches at the synapse emerge from receptor and kinase traffic. PLoS Comput Biol 2005; 1: 137–154
19 *Hemmings HC Jr*, *Greengard P*. DARPP-32, a dopamine- and adenosine 3′:5′-monophosphate-regulated phosphoprotein: regional, tissue, and phylogenetic distribution. J Neurosci 1986; 6: 1469–1481
20 *Hemmings HC Jr*, *Nairn AC*, *Greengard P*. DARPP-32, a dopamine- and adenosine 3′:5′-monophosphate-regulated neuronal phosphoprotein. II. Comparison of the kinetics of phosphorylation of DARPP-32 and phosphatase inhibitor 1. J Biol Chem 1984; 259: 14491–14497
21 *Hofmann F*, *Bechtel PJ*, *Krebs EG*. Concentrations of cyclic AMP-dependent protein kinase subunits in various tissues. J Biol Chem 1977; 252: 1441–1447
22 *Hyman SE*, *Malenka RC*. Addiction and the brain: the neurobiology of compulsion and its persistence. Nat Rev Neurosci 2001; 2: 695–703
23 *Hyman SE*, *Malenka RC*, *Nestler EJ*. Neural mechanisms of addiction: the role of reward-related learning and memory. Annu Rev Neurosci 2006; 29: 565–598
24 *Janowsky DS*, *Overstreet DH*. The role of acetylcholine mechanisms in mood disorders. In: Bloom FE, Kupfer DJ eds, Psychopharmacology: The fourth generation of progress. New York: Raven Press, Ltd; 1995, xlii+2002
25 *Kauer JA*. Learning mechanisms in addiction: synaptic plasticity in the ventral tegmental area as a result of exposure to drugs of abuse. Annu Rev Physiol 2004; 66: 447–475
26 *Kessler RC*, *Berglund P*, *Demler O et al*. The epidemiology of major depressive disorder: results from the National Comorbidity Survey Replication (NCS-R). Jama 2003; 289: 3095–3105
27 *Khantzian EJ*. The self-medication hypothesis of addictive disorders: focus on heroin and cocaine dependence. Am J Psychiatry 1985; 142: 1259–1264
28 *Kim M*, *Huang T*, *Abel T et al*. Temporal sensitivity of protein kinase a activation in late-phase long term potentiation. PLoS Comput Biol 2010; 6: e1000691
29 *Koob GF*, *Kenneth Lloyd G*, *Mason BJ*. Development of pharmacotherapies for drug addiction: a Rosetta stone approach. Nat Rev Drug Discov 2009; 8: 500–515
30 *Krystal JH*. N-methyl-D-aspartate glutamate receptor antagonists and the promise of rapid-acting antidepressants. Arch Gen Psychiatry 2010; 67: 1110–1111
31 *Lindskog M*, *Kim M*, *Wikstrom MA et al*. Transient calcium and dopamine increase PKA activity and DARPP-32 phosphorylation. PLoS Comput Biol 2006; 2: e119
32 *Luscher B*, *Shen Q*, *Sahir N*. The GABAergic deficit hypothesis of major depressive disorder. Mol Psychiatry 2010
33 *Maletic V*, *Robinson M*, *Oakes T et al*. Neurobiology of depression: an integrated view of key findings. International journal of clinical practice 2007; 61: 2030–2040
34 *Markou A*, *Kosten TR*, *Koob GF*. Neurobiological similarities in depression and drug dependence: a self-medication hypothesis. Neuropsychopharmacology 1998; 18: 135–174
35 *Mayberg HS*. Limbic-cortical dysregulation: a proposed model of depression. J Neuropsychiatry Clin Neurosci 1997; 9: 471–481
36 *Mayberg HS*. Defining the neural circuitry of depression: Strategies toward treatment selection based on neuroimaging phenotypes. Psychiatric Annals 2006; 36: 259–268
37 *Mayberg HS*. Targeted electrode-based modulation of neural circuits for depression. J Clin Invest 2009; 119: 717–725
38 *Monk CS*, *Klein RG*, *Telzer EH et al*. Amygdala and nucleus accumbens activation to emotional facial expressions in children and adolescents at risk for major depression. Am J Psychiatry 2008; 165: 90–98
39 *Murray CJ*, *Lopez AD*. Global mortality, disability, and the contribution of risk factors: Global Burden of Disease Study. Lancet 1997; 349: 1436–1442
40 *Nagase T*, *Murakami T*, *Nozaki H et al*. Tissue and subcellular distributions, and characterization of rat brain protein phosphatase 2A containing a 72-kDa delta/B" subunit. J Biochem 1997; 122: 178–187
41 *Nakano T*, *Doi T*, *Yoshimoto J et al*. A kinetic model of dopamine- and calcium-dependent striatal synaptic plasticity. PLoS Comput Biol 2010; 6: e1000670
42 *Nestler EJ*, *Carlezon WA Jr*. The mesolimbic dopamine reward circuit in depression. Biol Psychiatry 2006; 59: 1151–1159
43 *Nishi A*, *Bibb JA*, *Snyder GL et al*. Amplification of dopaminergic signaling by a positive feedback loop. Proc Natl Acad Sci USA 2000; 97: 12840–12845
44 *Ouimet CC*, *da Cruz e Silva EF*, *Greengard P*. The alpha and gamma 1 isoforms of protein phosphatase 1 are highly and specifically concentrated in dendritic spines. Proc Natl Acad Sci USA 1995; 92: 3396–3400
45 *Patel S*, *Morris SA*, *Adkins CE et al*. Ca2+-independent inhibition of inositol trisphosphate receptors by calmodulin: redistribution of calmodulin as a possible means of regulating Ca2+ mobilization. Proc Natl Acad Sci USA 1997; 94: 11627–11632
46 *Pelizza L*, *Ferrari A*. Anhedonia in schizophrenia and major depression: state or trait? Ann Gen Psychiatry 2009; 8: 22
47 *Price JL*, *Drevets WC*. Neurocircuitry of mood disorders. Neuropsychopharmacology 2010; 35: 192–216
48 *Qi Z*, *Miller GW*, *Voit EO*. Computational systems analysis of dopamine metabolism. PLoS One 2008; 3: e2444
49 *Qi Z*, *Miller GW*, *Voit EO*. A mathematical model of presynaptic dopamine homeostasis: implications for schizophrenia. Pharmacopsychiatry 2008; 41 (Suppl. 1): S89–S98
50 *Qi Z*, *Miller GW*, *Voit EO*. The internal state of medium spiny neurons varies in response to different input signals. BMC Syst Biol 2010; 4: 26
51 *Raison CL*, *Capuron L*, *Miller AH*. Cytokines sing the blues: inflammation and the pathogenesis of depression. Trends Immunol 2006; 27: 24–31
52 *Rakhilin SV*, *Olson PA*, *Nishi A et al*. A network of control mediated by regulator of calcium/calmodulin-dependent signaling. Science 2004; 306: 698–701
53 *Rao U*, *Hammen CL*, *Poland RE*. Mechanisms underlying the comorbidity between depressive and addictive disorders in adolescents: interactions between stress and HPA activity. The American journal of psychiatry 2009; 166: 361–369
54 *Rayport SG*, *Kandel ER*. Development of plastic mechanisms related to learning at identified chemical synaptic connections in Aplysia. Neuroscience 1986; 17: 283–294
55 *Reynolds JN*, *Hyland BI*, *Wickens JR*. A cellular mechanism of reward-related learning. Nature 2001; 413: 67–70
56 *Reynolds JN*, *Wickens JR*. Substantia nigra dopamine regulates synaptic plasticity and membrane potential fluctuations in the rat neostriatum, *in vivo*. Neuroscience 2000; 99: 199–203
57 *Reynolds JN*, *Wickens JR*. Dopamine-dependent plasticity of corticostriatal synapses. Neural Netw 2002; 15: 507–521
58 *Ross HE*, *Glaser FB*, *Germanson T*. The prevalence of psychiatric disorders in patients with alcohol and other drug problems. Arch Gen Psychiatry 1988; 45: 1023–1031
59 *Ross HE*, *Glasser FB*, *Stiasny S*. Sex differences in the prevalence of psychiatric disorders in patients with alcohol and drug problems. Br J Addict 1988; 83: 1179–1192
60 *Sanacora G*, *Mason GF*, *Rothman DL et al*. Reduced cortical gamma-aminobutyric acid levels in depressed patients determined by proton magnetic resonance spectroscopy. Arch Gen Psychiatry 1999; 56: 1043–1047
61 *Sanderson WC*, *Beck AT*, *Beck J*. Syndrome comorbidity in patients with major depression or dysthymia: prevalence and temporal relationships. Am J Psychiatry 1990; 147: 1025–1028
62 *Shi SH*, *Hayashi Y*, *Petralia RS et al*. Rapid spine delivery and redistribution of AMPA receptors after synaptic NMDA receptor activation. Science 1999; 284: 1811–1816
63 *Sim AT*, *Ratcliffe E*, *Mumby MC et al*. Differential activities of protein phosphatase types 1 and 2A in cytosolic and particulate fractions from rat forebrain. J Neurochem 1994; 62: 1552–1559
64 *Snyder GL*, *Allen PB*, *Fienberg AA et al*. Regulation of phosphorylation of the GluR1 AMPA receptor in the neostriatum by dopamine and psychostimulants in vivo. J Neurosci 2000; 20: 4480–4488
65 *Stahl SM*. Stahl's Essential Psychopharmacology: Neuroscientific Basis and Practical Applications. 3rd edition ed: Cambridge University Press; 2008; 1132
66 *Sulzer D*, *Sonders MS*, *Poulsen NW et al*. Mechanisms of neurotransmitter release by amphetamines: a review. Prog Neurobiol 2005; 75: 406–433
67 *Takahashi S*, *Ohshima T*, *Cho A et al*. Increased activity of cyclin-dependent kinase 5 leads to attenuation of cocaine-mediated dopamine signaling. Proc Natl Acad Sci USA 2005; 102: 1737–1742

68 *Tang K*, *Low MJ*, *Grandy DK et al*. Dopamine-dependent synaptic plasticity in striatum during in vivo development. Proc Natl Acad Sci USA 2001; 98: 1255–1260
69 *Tisch S*, *Silberstein P*, *Limousin-Dowsey P et al*. The basal ganglia: anatomy, physiology, and pharmacology. Psychiatr Clin North Am 2004; 27: 757–799
70 *Usui H*, *Inoue R*, *Tanabe O et al*. Activation of protein phosphatase 2A by cAMP-dependent protein kinase-catalyzed phosphorylation of the 74-kDa B" (delta) regulatory subunit in vitro and identification of the phosphorylation sites. FEBS Lett 1998; 430: 312–316
71 *Voit EO*. Computational analysis of biochemical systems: a practical guide for biochemists and molecular biologists. Cambridge, UK: Cambridge University Press; 2000, xii, 531 p.
72 *Voit EO*, *Qi Z*, *Miller GW*. Steps of modeling complex biological systems. Pharmacopsychiatry 2008; 41 (Suppl. 1): S78–S84
73 *Weiss RD*, *Mirin SM*, *Griffin ML*. Methodological considerations in the diagnosis of coexisting psychiatric disorders in substance abusers. Br J Addict 1992; 87: 179–187
74 *Wickens JR*, *Begg AJ*, *Arbuthnott GW*. Dopamine reverses the depression of rat corticostriatal synapses which normally follows high-frequency stimulation of cortex *in vitro*. Neuroscience 1996; 70: 1–5
75 *Willner P*. Dopamine and depression: a review of recent evidence. I. Empirical studies. Brain Res 1983; 287: 211–224
76 *Willner P*. Dopamine and depression: a review of recent evidence. II. Theoretical approaches. Brain Res 1983; 287: 225–236
77 *Willner P*. Dopamine and depression: a review of recent evidence. III. The effects of antidepressant treatments. Brain Res 1983; 287: 237–246
78 *Zetterstrom T*, *Sharp T*, *Ungerstedt U*. Further evaluation of the mechanism by which amphetamine reduces striatal dopamine metabolism: a brain dialysis study. Eur J Pharmacol 1986; 132: 1–9

Appendix

Reactions, kinetics, and initial conditions in the mathematical model of signal transduction and trafficking of AMPA receptors

All reactions are represented in the form of an enzymatic reaction or a simple binding reaction, with K_f denoting the rate constant for the forward process, K_b denoting the rate constant for the backward process, and K_c denoting the rate constant for the catalytic step in a Michaelis-Menten kinetics.

Table 1 Reactions and rate constants of signal transduction for DARPP-32 phosphorylation in dendrites of medium spiny neurons in the striatum (see legend of **Fig. 2c** for abbreviations).

Reaction	K_f ($nM^{-1}.s^{-1}$)#	K_b (s^{-1})	K_c (s^{-1})	Ref.
D1 + DA ↔ D1_DA	1.1E−3	10.0		[31]
D1_DA + $G_{\alpha\beta\gamma}$ ↔ D1_DA_$G_{\alpha\beta\gamma}$	6.0E−4	1.0E−3		[31]
D1 + $G_{\alpha\beta\gamma}$ ↔ D1_$G_{\alpha\beta\gamma}$	6.0E−5	3.0E−4		[31]
D1_$G_{\alpha\beta\gamma}$ + DA ↔ D1_DA_$G_{\alpha\beta\gamma}$	3.3E−3	10.0		[31]
D1_DA_$G_{\alpha\beta\gamma}$ → D1_DA + $G_\alpha GTP$ + $G_{\beta\gamma}$	20.0[a]			[31]
$G_\alpha GTP$ → $G_\alpha GDP$	10.0[a]			[31]
$G_\alpha GDP$ + $G_{\beta\gamma}$ → $G_{\alpha\beta\gamma}$	100.0			[31]
$G_\alpha GTP$ + AC5 ↔ $G_\alpha GTP$_AC5	3.9E−2	50.0		[31]
$G_\alpha GTP$_AC5 + ATP ↔ $G_\alpha GTP$_AC5_ATP	1.3E−4	2.6E−1		[31]
$G_\alpha GTP$_AC5_ATP ↔ $G_\alpha GTP$_AC5 + cAMP	28.5[a]	2.6E−4[b]		[31]
PKA + 2 cAMP ↔ PKA_$cAMP_2$	3.5E−8[c]	6.0E−2		[41]
PKA_$cAMP_2$ + 2 cAMP ↔ PKA_$cAMP_4$	2.7E−5[c]	0.28		[41]
PKA_$cAMP_4$ ↔ 2 PKAc + PKAr	0.05[a]	8.5E−8[c]		[41]
PDE1 + cAMP ↔ PDE1_cAMP → PDE1 + AMP	2.0E−3	72.0	18.0	[31]
PDE4 + cAMP ↔ PDE4_cAMP → PDE4 + AMP	2.0E−3	72.0	18.0	[31]
PKAc + PDE1 ↔ PKAc_PDE1 → PKAc + PDE1p	6.0E−3	36.0	9.0	[4]
PDE1p → PDE1	1.0E−1[a]			[4]
PKAc + PDE4 ↔ PKAc_PDE4 → PKAc + PDE4p	6.0E−3	36.0	9.0	[4]
PDE4p → PDE4	1.0E−1[a]			[4]
→ Ca^{2+}	1.0E+2[e]			[4]
Ca^{2+} →	2.0[a]			[4]
2 Ca^{2+} + PP2Bi ↔ PP2Bi_Ca_2	6.0E−3	0.91		[4]
2 Ca^{2+} + PP2Bi_Ca_2 ↔ PP2B	0.1	10.0		[4]
AC5 + Ca^{2+} ↔ AC5_Ca	1.0E−3	0.9		[31]
$G_\alpha GTP$ + AC5_Ca ↔ $G_\alpha GTP$_AC5_Ca	1.9E−2	25.0		[31]
$G_\alpha GTP$_AC5_Ca + ATP ↔ $G_\alpha GTP$_AC5_Ca_ATP	6.0E−5	1.3E−1		[31]
$G_\alpha GTP$_AC5_Ca_ATP ↔ $G_\alpha GTP$_AC5_Ca + cAMP	14.2[a]	1.3E−4[b]		[31]
PP2A + 4 Ca^{2+} ↔ PP2Ac	7.7E−12[d]	1.0E−2		[31]
PP2A + PKAc ↔ PP2A_PKAc → PP2Ap + PKAc	2.5E−3	0.3	0.1	[70]
PP2Ap → PP2A	4.0E−3[a]			[31]
CK1 → CK1p	1.0[a]			[14]
PP2B + CK1p ↔ PP2B_CK1p → PP2B + CK1	3.0E−2	24.0	6.0	[14]
CDK5 + Ca^{2+} ↔ CDK5c	3.0E−3	1.0		
PDE1p + cAMP ↔ PDE1p_cAMP → PDE1p + AMP	5.0E−3	80.0	20.0	
PDE4p + cAMP ↔ PDE4p_cAMP → PDE4p + AMP	5.0E−3	80.0	20.0	

[a]: Unit in s^{-1} ; [b]: Unit in $nM^{-1}.s^{-1}$; [c]: Unit in $nM^{-2}.s^{-1}$; [d]: Unit in $nM^{-4}.s^{-1}$; [e]: Unit in $nM.s^{-1}$

#: For a chemical reaction, K_f is the rate constant for the forward process, K_b is the rate constant for the backward process, while K_c is the rate constant for the catalytic step in a Michaelis-Menten kinetics

Table 2 Reactions and rate constants of DARPP-32 phosphorylation in dendrites of medium spiny neurons in the striatum (see legend of **Fig. 2c** for abbreviations).

Reaction	K_f ($nM^{-1}.s^{-1}$)[#]	K_b (s^{-1})	K_c (s^{-1})	Ref.
D + PKAc ↔ D_PKAc → D34 + PKAc	2.7E−3	8.0	2.0	[31]
D34 + PP2B ↔ D34_PP2B → D + PP2B	1.0E−2	2.0	0.5	[31]
D + CDK5 ↔ D_CDK5 → D75 + CDK5	4.5E−4	2.0	0.5	[31]
D75 + PP2Ap ↔ D75_PP2Ap → D + PP2Ap	4.0E−4	12.0	3.0	[31]
D75 + PP2Ac ↔ D75_PP2Ac → D + PP2Ac	4.0E−4	12.0	3.0	[31]
D + CK2 ↔ D_CK2 → D102 + CK2	4.0E−4	6.4	1.6	[17]
D102 → D	1.6[a]			
D + CK1 ↔ D_CK1 → D137 + CK1	4.4E−3	12.0	3.0	[67]
D137 + PP2C ↔ D137_PP2C → D + PP2C	7.5E−3	12.0	3.0	[14]
D34 + PP1 ↔ D34_PP1	1.0E−2	1.0		[14]
D34_PP1 + PP2B ↔ D34_PP1_PP2B → D + PP1 + PP2B	1.0E−3	2.0	0.5	[14]
D75 + PKAc ↔ D75_PKAc	4.6E−3	2.4		[5]
D + CDK5c ↔ D_CDK5c → D75 + CDK5c	1.8E−3	4.0	1.0	
2 Ca^{2+} + CaM ↔ Ca_2CaM	6.0E−3[b]	9.1		[31]
2 Ca^{2+} + Ca_2CaM ↔ Ca_4CaM	0.1[b]	1.0E+3		[31]
CaMKII + Ca_4CaM ↔ CaMKII_Ca_4CaM	0.01	0.8		[31]
CaMKII_Ca_4CaM → CaMKIIp + Ca_4CaM	5.0E−3[a]			[31]
CaMKIIp + PP1 ↔ CaMKIIp_PP1 → CaMKII + PP1	1.0E−4	1.4	0.35	[28, 31]
PKAc + I1 ↔ PKAc_I1 → PKAc + I1p	1.4E−3	5.6	1.4	[28, 31]
PP1 + I1p ↔ PP1_I1p	1.0E−3	5.0E−3		
PP2B + I1p ↔ PP2B_I1p → PP2B + I1	3.8E−3	12.0	3.0	

[a]: Unit in s^{-1} ; [b]: Unit in $nM^{-1}.s^{-1}$; [c]: Unit in $nM^{-2}.s^{-1}$; [d]: Unit in $nM^{-4}.s^{-1}$; [e]: Unit in $nM.s^{-1}$

[#]: For a chemical reaction, K_f is the rate constant for the forward process, K_b is the rate constant for the backward process, while K_c is the rate constant for the catalytic step in a Michaelis-Menten kinetics

Table 3 Reactions and rate constants of AMPAR trafficking, AMPAR phosphorylation, and AMPAR dephosphorylation in the postsynapse of striatal projection neurons (see legend of **Fig. 2c** for abbreviations).

Reaction	K_f ($nM^{-1}.s^{-1}$)	K_b (s^{-1})	K_c (s^{-1})	Ref.
cAMPAR + PKAc ↔ cAMPAR_PKAc → cAMPAR_Ser845p + PKAc	2.5E−3	4.0	1.0	[41]
cAMPAR_Ser845p + PP1 ↔ cAMPAR_Ser845p_PP1 → cAMPAR + PP1	5.0E−4	12.0	3.0	[64]
cAMPAR_Ser845p + PP2Ap ↔ cAMPAR_Ser845p_PP2Ap → cAMPAR + PP2Ap	1.7E−4	12.0	3.0	[64]
cAMPAR_Ser845p + PP2Ac ↔ cAMPAR_Ser845p_PP2Ac → cAMPAR + PP2Ac	1.7E−4	12.0	3.0	[64]
cAMPAR_Ser845p + CaMKIIp ↔ cAMPAR_Ser845p_CaMKIIp → cAMPAR_Ser845p_Ser831p + CaMKIIp	1.0E−4	2.0	0.5	[41]
cAMPAR_Ser845p_Ser831p + PP1 ↔ cAMPAR_Ser845p_Ser831p_PP1 → cAMPAR_Ser845p + PP1	5.0E−4	4.0	1.0	[64]
cAMPAR_Ser845p_Ser831p + PP2Ap ↔ cAMPAR_Ser845p_Ser831p_PP2Ap → cAMPAR_Ser845p + PP2Ap	1.7E−4	4.0	1.0	[64]
cAMPAR_Ser845p_Ser831p + PP2Ac ↔ cAMPAR_Ser845p_Ser831p_PP2Ac → cAMPAR_Ser845p + PP2Ac	1.7E−4	4.0	1.0	[64]
mAMPAR + PKAc ↔ mAMPAR_PKAc → mAMPAR_Ser845p + PKAc	2.5E−3	4.0	1.0	[41]
mAMPAR_Ser845p + PP1 ↔ mAMPAR_Ser845p_PP1 → mAMPAR + PP1	5.0E−4	0.8	0.2	[64]
mAMPAR_Ser845p + CaMKIIp ↔ mAMPAR_Ser845p_CaMKIIp → mAMPAR_Ser845p_Ser831p + CaMKIIp	1.0E−4	2.0	0.5	[41]
mAMPAR_Ser845p_Ser831p + PP1 ↔ mAMPAR_Ser845p_Ser831p_PP1 → mAMPAR_Ser845p + PP1	5.0E−4	4.0	1.0	[64]
mAMPAR → cAMPAR + Anchor	0.8E−3[a]			[18]
cAMPAR_Ser845p_Ser831p + Anchor ↔ mAMPAR_Ser845p_Ser831p	1.0E−5	0.1		[18]
cAMPAR ↔ Bulk_cAMPAR	1[a]	1.8E−2		[18]
cAMPAR_Ser845p → Bulk_cAMPAR	2.0E−5[a]			[18]
cAMPAR_Ser845p_Ser831p → Bulk_cAMPAR	2.0E−5[a]			[18]

[a]: Unit in s^{-1}

[#]: For a chemical reaction, K_f is the rate constant for the forward process, K_b is the rate constant for the backward process, while K_c is the rate constant for the catalytic step in a Michaelis-Menten kinetics

Table 4 Initial values for the DARPP-32 phosphorylation system in dendrites of medium spiny neurons in the striatum (see legend of **Fig. 2c** for abbreviations).

Molecule	Concentration (nM)	Reference
DA	10.0	[31]
D1	5.0E+2	[31]
$G_{\alpha\beta\gamma}$	3.0E+3	[31]
AC5	2.5E+3	[31]
ATP	2.0E+6	[31]
PDE1	5.0E+2	[31]
PDE4	5.0E+2	[31]
DARPP-32	3.0E+4	[19]
PKA	6.6E+3	[21]
PP2Bi	4.0E+3	[31]
CDK5	1.2E+3	[31]
PP2A	8.0E+2	[40, 63]
CK1	2.0E+3	
PP2C	2.0E+3	
PP1	2.3E+3	[11, 44]
CK2	2.0E+3	
Anchor	11.56E+3	[41]
Bulk_cAMPAR	6.0E+3	[41]
CaM	1.0E+4	[45, 52]
CaMKII	2.0E+4	[31]
I1	1.0E+3	